

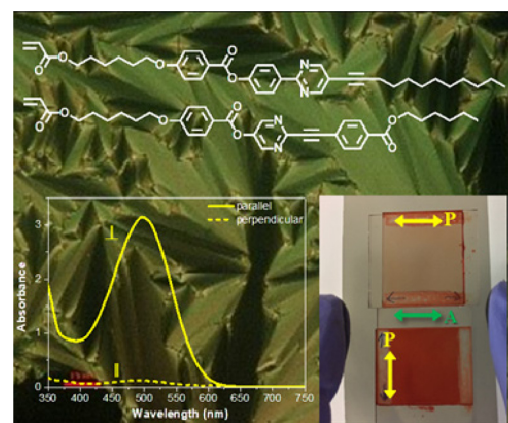
Syntheses and Properties of New Smectic Reactive Mesogens and Their Application in Guest-Host Polarizer

Yang Ye¹
Rui He^{1,2}
Eunche Oh¹
Shin-Woong Kang²
Seung Hee Lee²
Xiang-Dan Li³
Myong-Hoon Lee^{*1}

¹ Graduate School of Flexible and Printable Electronics, Jeonbuk National University, Jeonju, 54896, Korea
² Department of BIN convergence Technology, Jeonbuk National University, Jeonju, 54896, Korea
³ Key Laboratory of Catalysis and Materials Science of the State Ethnic Affairs Commission & Ministry of Education, South-Central University for Nationalities, Wuhan, Hubei 430074, P. R. China

Received November 18, 2019 / Revised March 19, 2020 / Accepted May 8, 2020

Abstract: We designed and synthesized new smectic liquid crystalline monomers containing photopolymerizable acrylate groups and a mesogenic core unit composed of two benzene rings, one pyrimidine-based heteroaromatic ring and an acetylene linking group. The structures of monomers were characterized by ¹H nuclear magnetic resonance spectroscopy, and their mesomorphic behaviors were investigated by differential scanning calorimetry and polarized optical microscopy. Both of monomers showed an enantiotropic phase transition behavior with exhibiting both nematic phase and highly ordered smectic phase. Both of monomers showed smectic phases during the cooling process in the temperature range of 144.2–94.0 °C and 154.0–85.8 °C, respectively. Neither of these compounds showed a homogeneous alignment even at various temperatures, and therefore, their 50:50 mixture was chosen for the preparation of guest-host mixture because of its lowest crystallization point, wide smectic phase temperature range and superior aligning property. Polymerizable “host-guest” mixture formulated from the host liquid crystalline monomer mixture, dichroic dye and additives was injected into the sandwiched glass substrates having rubbed alignment layers at the isotropic temperature. Subsequent *in-situ* photopolymerization by UV irradiation at room temperature successfully resulted in a thin film polarizer with good polarizing properties. The fabricated guest-host polarizer showed a dichroic ratio (DR) of 13.1 and a degree of polarization (DOP) of 95.5% with the thickness of 5 μm.



Keywords: reactive mesogen, smectic phase, *in-situ* polymerization, host-guest system, coatable polarizer.

1. Introduction

Polarizer is one of the basic and indispensable optical components in the current display devices such as liquid crystal displays (LCDs) and organic light emitting displays (OLEDs).¹ The polarizer can be defined as an optical filter that lets light waves of a specific polarization pass through while blocking light waves of other polarizations.² Not only being used as a light control valve in LCDs, linear polarizers have been widely used in various fields such as sensors, optofluidic components, and optoelectronics. Especially, they become an indispensable component in the flexible OLED display, because an anti-reflection film can be fabricated by combining a $\lambda/4$ retarder film and a linear polarizer.³

Acknowledgments: This work was supported by the Basic Science Research Program through the National Research Foundation of Korea (NRF) funded by the Ministry of Education (2018R1D1A1B07044250) and by Korea Institute for Advancement of Technology (KIAT) grant funded by the Korea Government (MOTIE) (P0002007, The Competency Development Program for Industry Specialist). MHL thanks to the financial support from the Polymer Materials Fusion Research Center and the research funds of Chonbuk National University in 2018.

*Corresponding Author: Myong-Hoon Lee (mhlee2@jbnu.ac.kr)

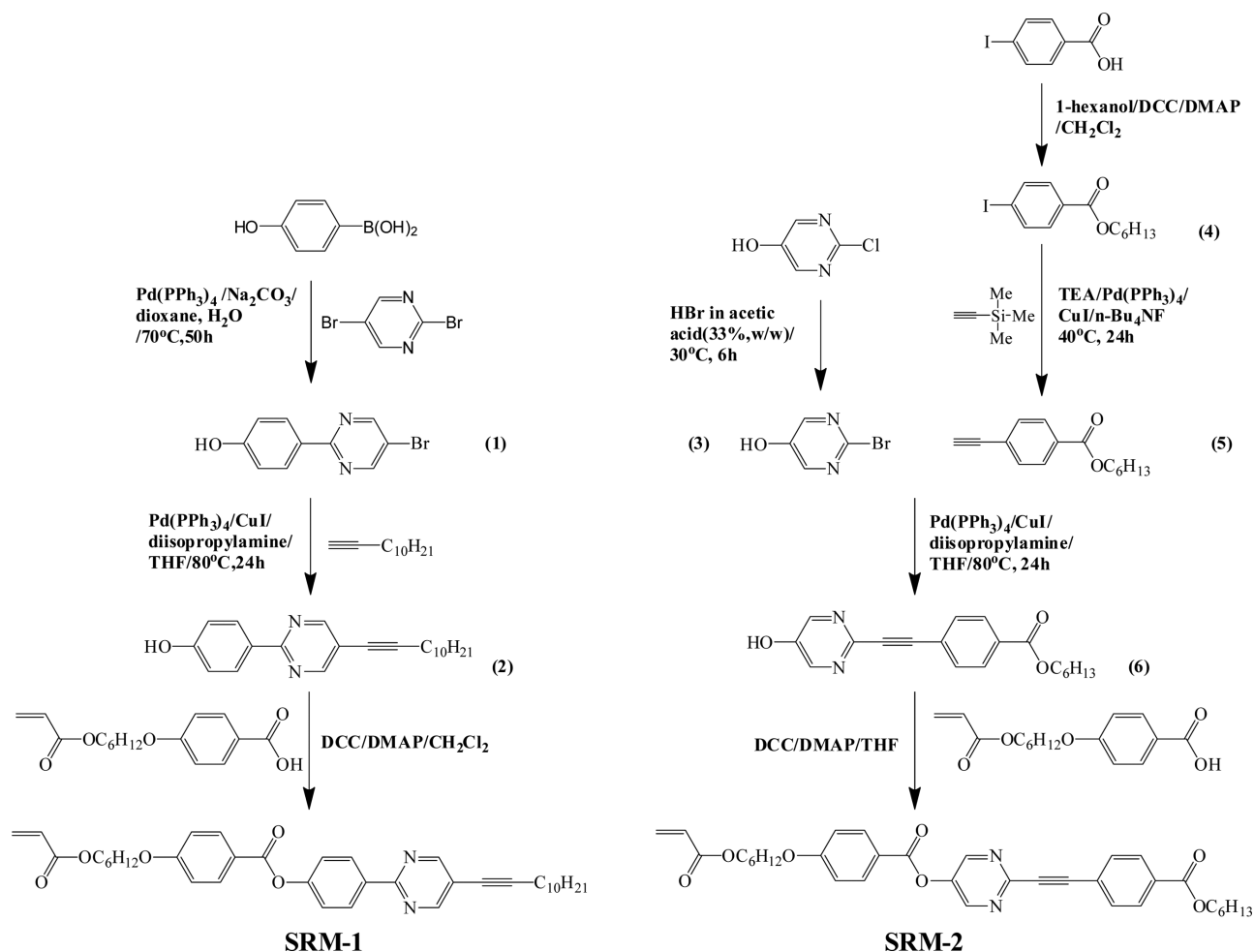
Currently, the most commonly used polarizers for display applications are derivatives of H-sheet polarizer, which was invented by E. H. Land in 1938.⁴ The dichroism of these polarizers is achieved by highly ordered absorbing materials of iodine complexes, which are uniaxially aligned by stretched polyvinyl alcohol (PVA) sheet with addition of boric acid.^{5,6} As incident light passing through these sheet polarizers, the light polarization parallel to iodine molecular wires is absorbed while the polarization perpendicular to iodine molecular wires is transmitted to achieve an optically anisotropic transmittance.^{6–9} These H-sheet polarizers show excellent optical performances such as high single transmittance and high polarization efficiency. However, two triacetylcellulose (TAC) layers are needed to protect PVA layer from moisture and sublimation of iodine molecules. Furthermore, an adhesive release film is attached on the bottom of the H-sheet polarizer for the lamination of the polarizer to the LCD panel. These additional protective and adhesive films add unnecessary layer thickness to the sheet polarizers with low solvent resistance. In addition, these conventional polarizers still have several limitations such as inferior heat and moisture stability, and bending or distortion issues derived from the stretching-induced residual stress.^{10,11} Due to these reasons, the conventional PVA/

iodine polarizers are not suitable for applications in the state-of-the-art display technologies such as ultra-thin LCDs or flexible displays in recent years.¹²⁻¹⁴

To overcome such drawbacks, the concept of coatable polarizer with ultra-thin thickness has been developed. The thin coatable polarizer not only shows significant reduction in thickness but also can be assembled inside of the cell to eliminate the parallax-related issues.¹⁵ Moreover, when the novel coatable polarizers act as the internal polarizers (in-cell polarizers), the fabrication of LCD devices can be based on thin, light-weight and flexible plastic substrates as well as cheap, low-quality glass substrates, which allows for a number of additional degrees of freedom in the optical design of LCDs.¹⁶⁻¹⁹

Among various fabrication methods, the thin-film polarizers based on dichroic guest-host system offer numerous advantages over traditional sheet polarizer, such as reduced thickness and weight, and the in-cell application in LCDs can be achieved and may play a role in the development of flexible displays.^{15,17,20,21} In this method, anisotropic absorption of visible light can be achieved by co-aligning "guest" dichroic dye molecules along with highly ordered polymerizable "host" liquid crystal molecules, also known as reactive mesogens (RMs). While the low viscosity of RMs enabled an easy alignment by alignment layer, the subsequent *in-situ* polymerization provided a freedom to immobilize the optimum phase and molecular ordering.^{15,17} It is also well known that, among various polymerizable liquid

crystalline compounds, RMs having a smectic phase are most efficient to obtain a high dichroic ratio (DR).¹⁵ Compared to the RMs in the nematic phase which retains only a statistically parallel arrangement of molecules (orientational order), the RMs in smectic phase possess a lamellar arrangement of molecules beyond orientational order.²² In smectic guest-host systems, therefore, the "guest" dichroic dye molecules can have higher ordering than those of nematic phase. On this basis, a series of new liquid crystalline reactive monomers with smectic phases were designed and synthesized. Recently, we also have reported the synthesis of novel RM based on diphenylacetylene (tolane) structure and its utilization for the fabrication of guest-host type ultra-thin coatable polarizer on a single substrate.²³ *In-situ* photopolymerization of the thin film containing tolane-based RM and dichroic dye successfully resulted in a coatable polarizer with good polarizing properties. The fabricated coatable polarizer showed a dichroic ratio (DR) of 16.4 and a degree of polarization (DOP) of 99.3% with the thickness of 4 μm . The resulting coatable polarizer possessed a considerable solvent resistance, good thermal stability and robust mechanical properties. However, despite the various advantages and possible applications of coatable polarizers, some drawbacks such as low optical properties and complicated film fabrication processes should be overcome prior to the commercialization. In addition, there are difficulties to achieve highly efficient optical performances such as dichroic ratio and polarization efficiency, because only a limited number of RMs are



Scheme 1. Structures and synthetic schemes for smectic RMs.

known to have a smectic phase at the room temperature up to date.

In this paper, we designed and synthesized the new RMs having a highly ordered smectic mesophase at an appropriate temperature range, of which the structures and syntheses are schematically displayed in Scheme 1. The new monomers or their mixtures should possess a low viscosity in a nematic phase to form a homogeneously aligned mono-domain within the cell during the alignment process, and ability to form a highly ordered smectic phase upon further cooling. We characterized the structures and their mesomorphic properties of the RMs. The fabrication of thin coatable polarizers was demonstrated by using the synthesized RMs, and their optical performances were discussed.

2. Experimental

2.1. Materials

4-Hydrobenzenboronic acid, 2-chloro-5-pyrimidinol, 1-dodecyne, *N,N*-dimethylaniline, acryloyl chloride, 4-((6-(acryloyloxy)hexyl)oxy)benzoic acid, tetrakis(triphenylphosphine)palladium(0), *N,N'*-dicyclohexylcarbodiimide (DCC), 4-dimethylaminopyridine (DMAP), triethylamine, diisopropylamine, copper(I) iodide, HBr in acetic acid (33%, w/w), 4-iodobenzoic acid, 1-hexanol, trimethylsilylacetylene, 75% (w/w) tetrabutylammonium fluoride solution in water, methanesulfonic acid, and all other solvents were purchased from Sigma-Aldrich and used without further purification. MgSO₄, KI, HCl, Na₂CO₃, K₂CO₃, and NaHCO₃ were purchased from TCI Co. Azo-based dichroic red dye (DAD, λ_{\max} = 485 nm), as shown in Figure 1, was synthesized according to the procedure described in the literature.²³

2.2. Synthesis of SRM-1

2.2.1. Synthesis of 4-(5-bromopyrimidin-2-yl)phenol (1)

2,5-Dibromopyrimidine (1.000 g, 4.20 mmol) and 4-hydrobenzenboronic acid (0.580 g, 4.20 mmol) were dissolved in 1,4-dioxane (79.0 mL), and tetrakis(triphenylphosphine)palladium(0) (0.209 g, 0.18 mmol) was added. The mixture was stirred at 25 °C for 2 min. Aqueous Na₂CO₃ solution (11.0 mL, 1.0 M) was then added. The mixture was stirred for 50 h at 70 °C under nitrogen atmosphere, and then evaporated under vacuum. The residual solid was partially dissolved in ethyl acetate, and undissolved solid was filtered off. After concentration under vacuum, the crude product was purified by column chromatography on silica gel with tetrahydrofuran (THF)/hexane (1:2 v/v). After removing the solvent, the residual solid was dried in a vacuum oven at 40 °C overnight to give 0.50 g of compound **1** as white powder (Yield = 47%).

2.2.2. Synthesis of 4-(5-(dodec-1-yn-1-yl)pyrimidin-2-yl)phenol (2)

A mixture of phenol (1) (0.300 g, 1.19 mmol), 1-dodecyne (0.246 g, 1.43 mmol), diisopropylamine (0.34 mL), copper(I) iodide (0.011 g,

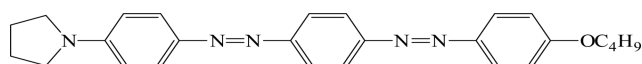


Figure 1. Chemical structure of DAD.

0.07 mmol) and tetrakis(triphenylphosphine)palladium (0) (0.083 g, 0.07 mmol) in 20 mL THF was stirred at 85 °C for 24 h under nitrogen atmosphere, and cooled to room temperature. After evaporating the solvent under vacuum, the residual solid was dissolved in dichloromethane. The mixture was filtered and concentrated under reduced pressure. The residue was purified by column chromatography on silica column with ethyl acetate/dichloromethane (1:10 v/v). The product was dried in a vacuum oven at room temperature overnight to obtain 0.32 g of compound **2** as yellow powder (Yield = 80%).

2.2.3 Synthesis of 4-(5-(dodec-1-yn-1-yl)pyrimidin-2-yl)phenyl 4-((6-(acryloyloxy)hexyl)oxy)benzoate (SRM-1)

To a mixture of 4-((6-(acryloyloxy)hexyl)oxy)benzoic acid (0.252 g, 0.86 mmol), compound **2** (0.290 g, 0.86 mmol) and DMAP (0.013 g, 0.01 mmol) in 15 mL of dichloromethane, 0.213 g of DCC (1.03 mmol) was added. The mixture was stirred at room temperature for 24 h. After cooling to room temperature, the mixture was filtered and concentrated at reduced pressure. The residual solution was purified by column chromatography on silica column with ethyl acetate/petroleum ether/dichloromethane (1:20:20 v/v) to yield crude product. The compound was dissolved in acetone, and then undissolved solid was filtered off by micro-filter. The analytically pure product (0.301 g, white crystal) was obtained by recrystallization from acetone (Yield = 57%).

¹H NMR (400 MHz, Chloroform-*d*) δ 8.76 (s, 2H), 8.50 (d, *J* = 8.7 Hz, 2H), 8.16 (d, *J* = 8.7 Hz, 2H), 7.34 (d, *J* = 8.7 Hz, 2H), 6.97 (d, *J* = 8.8 Hz, 2H), 6.41 (dd, *J* = 17.2, 1.1 Hz, 1H), 6.13 (dd, *J* = 17.3, 10.4 Hz, 1H), 5.82 (dd, *J* = 10.3, 1.2 Hz, 1H), 4.19 (t, *J* = 6.6 Hz, 2H), 4.06 (t, *J* = 6.4 Hz, 2H), 2.47 (t, *J* = 7.1 Hz, 2H), 1.85 (dt, *J* = 13.9, 6.5 Hz, 2H), 1.76 (d, *J* = 6.9 Hz, 1H), 1.70 (dd, *J* = 13.7, 6.9 Hz, 2H), 1.67 - 1.44 (m, 19H), 0.88 (t, *J* = 6.6 Hz, 3H).

2.3. Synthesis of SRM-2

2.3.1. Synthesis of 2-bromo-5-pyrimidinol (3)

A mixture of 2-chloro-5-pyrimidinol (5.000 g, 38.30 mmol) and HBr in acetic acid (33%, w/w) (50 mL) was stirred at 30 °C for 6 h, and the solvent was evaporated under vacuum. 4.488 g of compound **3** was obtained after recrystallization from *n*-hexane as a need crystal with 90% yield.

2.3.2. Synthesis of hexyl 4-iodobenzoate (4)

To a mixture of 4-iodobenzoic acid (4.960 g, 20.00 mmol), 1-hexanol (2.160 g, 21.00 mmol) and DMAP (0.250 g, 2.00 mmol) in 75 mL of dichloromethane, DCC (4.950 g, 24.00 mmol) was added, and the mixture was stirred at room temperature for 24 h. The solution was washed within water and dried by anhydrous MgSO₄. After the solvent evaporation, the mixture was purified by column chromatography on silica column with ethyl acetate/hexane (1:9 v/v) to obtain 4.720 g of compound **4** as colorless liquid (Yield = 71%).

2.3.3. Synthesis of hexyl 4-ethynylbenzoate (5)

To a mixture of hexyl 4-iodobenzoate (4) (3.320 g, 10.00 mmol), triethylamine (30 mL), copper(I) iodide (0.038 g, 0.20 mmol)

and tetrakis(triphenylphosphine) palladium (0) (0.231 g, 0.20 mmol), 1.470 g of trimethylsilylacetylene (15.00 mmol) was added with stirring under nitrogen atmosphere. After the mixture was stirred for 24 h at 40 °C, 4.8 mL of tetrabutylammonium fluoride solution in water (75% w/w) was added dropwise. After stirring for another 30 min, the solvent was evaporated under vacuum. The residual mixture was dissolved in 50 mL of dichloromethane and washed with a 0.5 M HCl aqueous solution. The organic phase was dried by anhydrous MgSO₄, filtered and evaporated. The residue was purified by column chromatography with dichloromethane/hexane (1:2 v/v) to obtain 1.270 g of compound 5 as a yellow solid (Yield = 55%).

2.3.4. Synthesis of hexyl 4-((5-hydroxypyrimidin-2-yl)ethynyl)benzoate (6)

A mixture of 2-bromo-5-pyrimidinol (3) (2.340 g, 13.40 mmol), hexyl 4-ethynylbenzoate (5) (3.400 g, 14.70 mmol), diisopropylamine (3.75 mL), copper(I) iodide (0.128 g, 0.67 mmol) and tetrakis(triphenylphosphine)palladium (0) (0.775 g, 0.67 mmol) in 134 mL of THF was stirred at 80 °C for 24 h under nitrogen atmosphere and then cooled to room temperature. After filtration, the residual mixture was concentrated under reduced pressure. The mixture was purified by column chromatography on silica column with THF/hexane (3:4 v/v). The product was obtained as a yellow powder (1.740 g) after solvent evaporation, and kept in a vacuum oven at room temperature until to be used (Yield = 40%).

2.3.5. Synthesis of hexyl-4-((5-((4-((6-acryloyloxy)hexyl)oxy)bezoyl)oxy)pyrimidin-2-yl)ethynyl)benzoate (SRM-2)

To a mixture of 4-((6-(acryloyloxy)hexyl)oxy)benzoic acid (0.721 g, 2.47 mmol), compound 6 (0.800 g, 2.47 mmol) and DMAP (0.036 g, 0.3 mmol) in 40 ml of dichloromethane, DCC (0.611 g, 2.96 mmol) was added. The mixture was stirred at room temperature for 24 h. After the mixture was filtered and concentrated, the residual solution was purified by column chromatography on silica column with ethyl acetate/petroleum ether/dichloromethane (2:11:11 v/v) to yield a crude product. The product was dissolved in acetone, and undissolved solid was filtered off by micro-filter. The product was recrystallized from acetone to obtain white crystal (0.80 g) in 54% yield.

¹H NMR (400 MHz, Chloroform-*d*) δ 8.77 (s, 2H), 8.19-8.10 (m, 2H), 8.10-8.02 (m, 2H), 7.77-7.70 (m, 2H), 7.03-6.96 (m, 2H), 6.41 (dd, *J* = 17.4, 1.5 Hz, 1H), 6.13 (dd, *J* = 17.3, 10.4 Hz, 1H), 5.83 (dd, *J* = 10.4, 1.5 Hz, 1H), 4.33 (t, *J* = 6.7 Hz, 2H), 4.19 (t, *J* = 6.7 Hz, 2H), 4.07 (t, *J* = 6.4 Hz, 2H), 1.92-1.67 (m, 6H), 1.59-1.41 (m, 6H), 1.35 (dq, *J* = 7.1, 3.6 Hz, 4H), 0.95-0.87 (m, 3H).

2.4. Characterization and measurements

2.4.1. Characterizations

¹H NMR spectra was recorded on JNM-AL400 FT/NMR spectrometer (400MHZ, JEOL Ltd., Japan in chloroform-*d* or DMSO-*d*₆. The detailed results are discussed in the next section. The mesomorphic behaviors of the synthesized RMs and the “host-guest” mixtures were studied by polarized optical microscopy (POM) and differential scanning calorimetry (DSC) at various temperatures. POM

experiment was carried out with Nikon ECLIPSE LV100 (Nikon Co., Japan) equipped with a Nikon DS-Ril digital camera DXM1200 and a heating hot-stage LINKAM controlled by temperature controller LINKAM T95-HS. DSC experiment was conducted on DSC 2010 differential scanning calorimeter (TA Instruments Inc., USA) at heating and cooling rates of 10 °C/min under nitrogen atmosphere. Phase transition temperatures were obtained from the onset temperature during heating and cooling processes.

2.4.2. Fabrication of thin-film polarizers

Azo-based dichroic dye DAD in Figure 1 was synthesized according to the literature,²³ and used as a guest material. Firstly, a series of RM mixtures was prepared by mixing appropriate amounts of SRM-1 and SRM-2 in different ratios (35:65, 50:50, and 65:35 wt/wt). The “guest-host” mixture was prepared by mixing the prepared RM mixture with 1.5 wt% of dichroic red dye (DAD), and 1.0 wt% of photo initiator (Irgacure® 369). 4-Methoxyphenol (0.2~0.3 wt%) was added as a radical inhibitor to prevent an unwanted thermal polymerization during the heating processes. The mixture was dissolved in dichloromethane completely and filtered using a micro-filter. After evaporating the solvent, the mixture was dried in vacuo for several hours to ensure complete removal of solvent. The mixture was injected into a sandwich cell of 5 μm gap containing rubbed anti-parallel alignment layers by capillary force at above the isotropic temperature of the mixture. The alignment layer was prepared by coating a conventional alignment layer (AL-16470, JSR Co.) on a glass substrate followed by a standard process of two-step baking and rubbing. The sandwich cell filled with the “guest-host” mixture was firstly heated above the isotropic temperature, followed by an annealing step at the nematic temperature of the mixture to obtain a uniform homogeneous alignment, and then, cooled to room temperature to obtain a uniformly aligned smectic phase. The *in-situ* photopolymerization was carried out at room temperature by irradiating UV light with an intensity of 10 mW/cm² (@365 nm) for a certain period of time to enable the stabilization of high ordered smectic phase.

2.5. Evaluation of polarizing properties

To evaluate polarizing properties of coatable polarizers in a sandwich cell, polarized UV-Vis spectra of the sandwich cell were obtained by using UV-vis spectrophotometer (S-3100, Scinco Co., Korea) with a Glan-Tylor rotating polarizer and a heating hot-stage LINKAM controlled by temperature controller LINKAM T95-HS. The guest-host mixtures were injected into the cells at above clearing point and then cooled to room temperature at a rate of 2 °C/min. Polarized UV-vis absorption at parallel and perpendicular direction to the liquid crystal director was recorded every 10 °C. The dichroic ratio (DR), order parameter (S) and the degree of polarization (DOP) were calculated from the equations as follows:²⁴

$$DR = \frac{A_{\parallel}}{A_{\perp}} \quad (1)$$

$$S = \frac{A_{\parallel} - A_{\perp}}{A_{\parallel} + A_{\perp}} = \frac{DR - 1}{DR + 2} \quad (2)$$

$$\text{DOP} = \frac{T_{\parallel} - T_{\perp}}{T_{\parallel} + T_{\perp}} \times 100\% \quad (3)$$

where A_{\parallel} and A_{\perp} are defined as the absorbance of the sample when the polarizer is parallel and perpendicular to the average orientation of long axis of dye chromophores, respectively. T_{\parallel} and T_{\perp} are defined as the transmittance of the sample when the polarizer is parallel and perpendicular to the average orientation of long axis of dye chromophores, respectively. For all the samples, DR, S, and DOP values were obtained by an average of 3 measurements to minimize the experimental errors.

3. Results and discussion

3.1. Structure characterizations of SRM-1 and SRM-2

In this work, two benzene rings, one pyrimidine-based heteroaromatic ring and an acetylene linking group are chosen as mesogenic core structure which allows for good lateral intermolecular interaction to generate smectic phase. Ester linkage as a linking group and long alkyl (decyl and hexyl) groups at both ends were also introduced to achieve a low viscosity and low phase transition temperatures. To obtain a smectic phase, the molecules should have constraints of layers stabilized by terminal long alkyl chains (R, R') that intertwine with each other. In these monomers, the terminal chains are linked to the mesogenic core unit by oxygen or acetylene. The structures of smectic RMs are illustrated in Scheme 1. SRM-1 is composed of pyrimidine-containing mesogenic core with an acetylene group on one side of core, whereas SRM-2 is composed of two aromatic cores, *i.e.*, one phenyl ring and one pyrimidine-containing aromatic ring, linked by an acetylene group. In both cases, an acryloyl group was attached at one end of alkyl terminal for polymerization.

The SRM-1 was prepared by convergent syntheses in which the final step was the esterification of 4-((6-(acryloyloxy)hexyl)oxy)benzoic acid and the corresponding phenol intermediate **2**. The esterification reaction was carried out by the Steglich/Hassner method using DCC and DMAP as catalysts at room temperature.²⁵⁻²⁷ The ¹H NMR spectra of SRM-1 was illustrated in Figure 2(a), and all the chemical shifts and integrations were matched well as marked in the figure. For SRM-2, the interme-

diolate **6** was firstly prepared by Sonogashira coupling reaction between reactant **5** and 2-bromo-5-pyrimidinol (**3**) as described in the synthetic route in Scheme 1.²⁸⁻³⁰ SRM-2 was prepared in the final step by the Steglich/Hassner esterification of 4-((6-(acryloyloxy)hexyl)oxy)benzoic acid and intermediate **6**. The successful synthesis of SRM-2 was also confirmed by ¹H NMR spectra, and all the detailed proton interpretations are also marked as shown in Figure 2(b).

3.2. Mesomorphic behavior of SRM-1 and SRM-2

SRM-1 and SRM-2 were subjected to be investigated by differential scanning calorimetry (DSC), and polarized optical microscopy (POM) at various temperatures. All the DSC measurements were carried out at a scanning rate of 10 °C/min, and the samples were sealed in aluminum pans with 200~300 ppm of thermal inhibitor (4-methoxyphenol) to protect from thermal polymerization. As-prepared powder samples were used for POM observation. DSC thermograms of SRM-1 and SRM-2 are displayed in Figure 3, and their phase transition behaviors are summarized in Table 1. POM images of SRM-1 and SRM-2 taken at various temperatures are also shown in Figure 4. Both of SRM-1 and SRM-2 showed an enantiotropic phase transition behavior. In the case of SRM-1, three exothermic peaks were observed during the heating and cooling processes, respectively. Upon cooling of the isotropic liq-

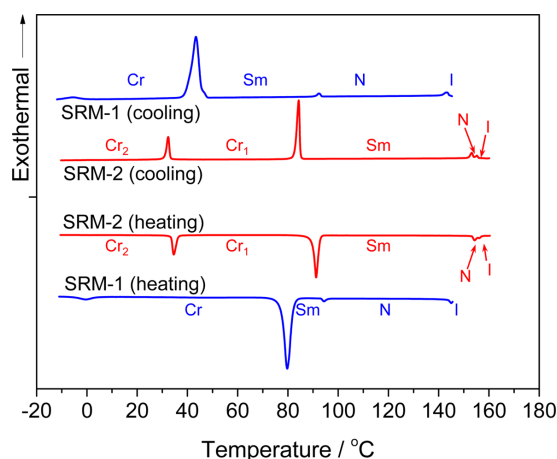


Figure 3. DSC thermograms of SRM-1 and SRM-2.

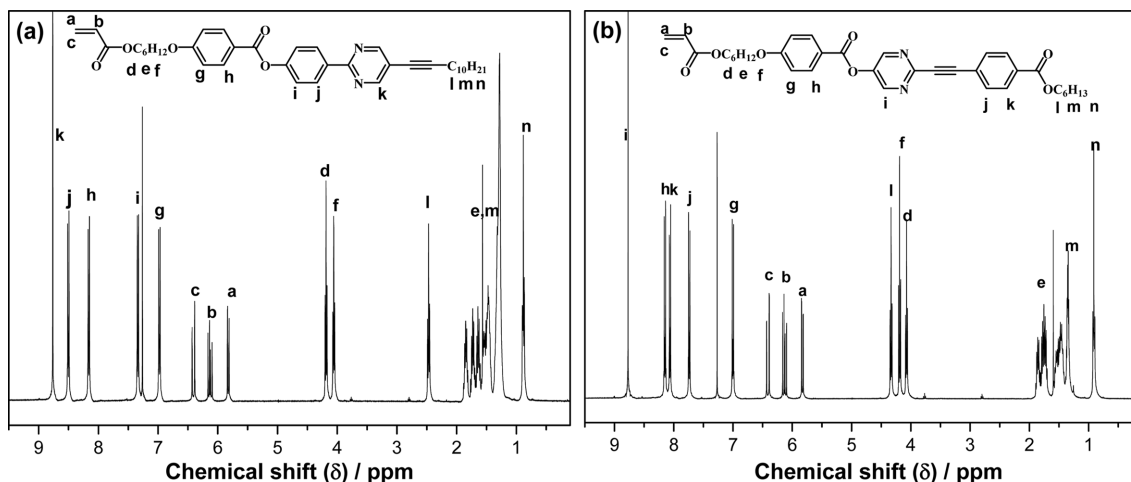
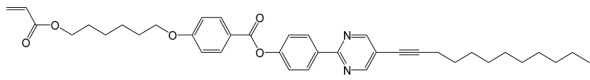
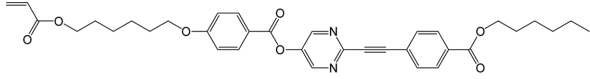


Figure 2. ¹H NMR spectra of (a) SRM-1 and (b) SRM-2.

Table 1. Phase transition temperatures of SRM-1 and SRM-2^a

SRM-1	
	Cooling (°C) I 144.2 N 94.0 Sm 47.8 Cr Heating (°C) Cr 74.2 Sm 93.3 N 143.1 I
SRM-2	
	Cooling (°C) I 155.9 N 154.0 Sm 85.8 Cr ₁ 33.9 Cr ₂ Heating (°C) Cr ₂ 32.1 Cr ₁ 85.7 Sm 152.6 N 155.8 I

^aI: Isotropic, N: Nematic, Sm: Smectic, Cr: Crystalline.

uid of SRM-1, a nematic phase was observed in the temperature range of 144.2–94.0 °C from the DSC, which can be also confirmed by POM image of fluid Schlieren texture (Figure 4(a)). Upon further cooling, however, no fan or mosaic optical texture was observed while a distinct phase transition was detected at 94.0 °C in the DSC thermogram. However, although the change of the texture was small, the transition can be observed from the POM as shown in Figure 4(b). We assume the phase between 94.0–47.8 °C to be a smectic phase because there was a distinct transition observed below the nematic phase from the DSC with a transition energy comparable to those observed in many cases for the nematic smectic transitions. In addition, pressing the cover glass with a needle caused a flow with strong light flashes in the POM. For instance, a texture similar to a nematic Schlieren texture has been previously observed with some smectic liquid, which was classified as smectic C or smectic B.³¹ For more clear identification of this phase, however, more sophisticated investigation should be necessary in the future. Upon further cooling, SRM-1 showed a transition to a crystalline phase at 47.8 °C. Although the crystallization temperature was still too high for the room temperature process, the smectic phase temperature range was relatively wide between 94.0 and 47.8 °C. Probably, this is due to the long alkyl chains at the termini which stabilized the lamellar pack-

ing with an excessive van der Waals intermolecular attraction.

In the case of SRM-2, a nematic phase was observed only in a very short temperature range followed by a smectic phase in the temperature range between 154.0 and 85.8 °C, and two crystalline phases below 85.8 °C. As shown in Figure 4, a fluid Schlieren texture was observed at 155.2 °C for a nematic phase, which was subsequently followed by a smectic phase in fan-shaped texture in the temperature range of 154.0 and 85.8 °C. It should be noted that SRM-2 exhibited a wide smectic phase range considering that the alkyl termini were hexyl (C₆) chains, which seems to be attributed to a longer mesogenic core containing a pyrimidine ring.

3.3. Fabrication and evaluations of guest-host thin film polarizers

We attempted to utilize either of the synthesized SRMs for the preparation of guest-host thin film polarizers. Firstly, each of the pure SRMs was injected into a sandwich cell containing rubbed anti-parallel alignment layers (AL-16470, JSR Co.) at above the isotropic temperature. The cell was annealed at the nematic temperature, and cooled down to room temperature. Unfortunately, neither of the SRMs showed a homogeneous alignment even at various temperatures. In the case of SRM-1, it is thought that the homogeneous alignment was obstructed by two directional orientations of SmC phase under planar anchoring.³² On the other hand, SRM-2 exhibits a high crystalline temperature, which could prevent the homogeneous alignment at near room temperature. Hence, mixing of SRM-1 and SRM-2 could be one of the approaches to achieve the purpose. SRM-1 and SRM-2 were mixed in different weight ratios (35:65, 50:50, 65:35), and the phase behaviors of the mixtures were studied by DSC and POM, as shown in Figure 5 and Figure 6. From the DSC, lower crystal point and wider smectic phase temperature range were detected in all mixtures as compared to those of either original SRMs. In the cooling process, while the nematic-to-smectic phase

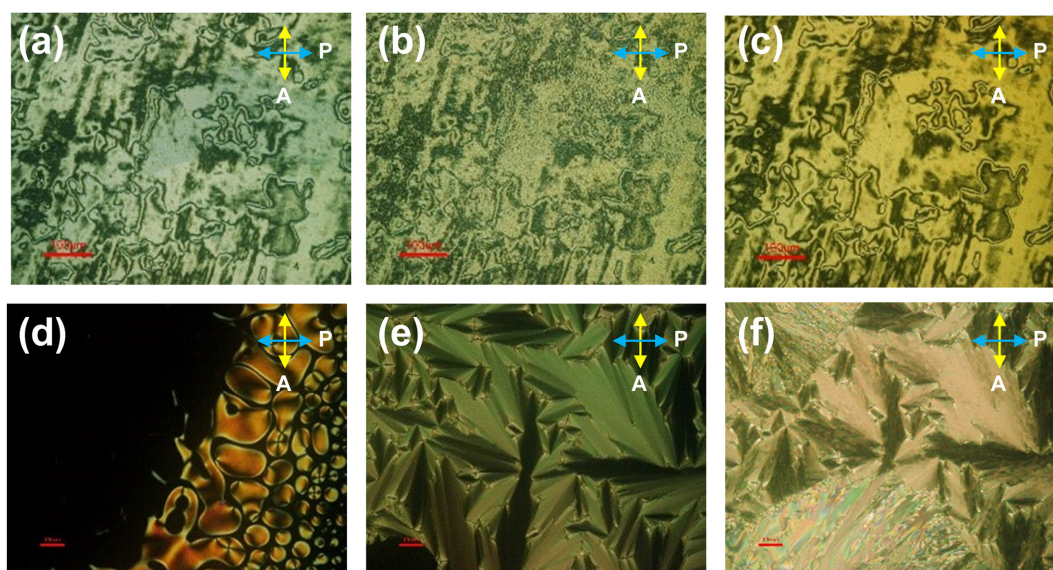


Figure 4. POM images of observed at various temperature during the cooling process (10 °C/min): (a) 113.0 °C (N), (b) 94.0 °C (N-Sm), and (c) 54.0 °C (Sm) for SRM-1; (d) 155.2 °C (N), (e) 119.4 °C (Sm), and (f) 82.0 °C (Cr) for SRM-2 (Samples were observed on a glass substrate with a cover glass.).

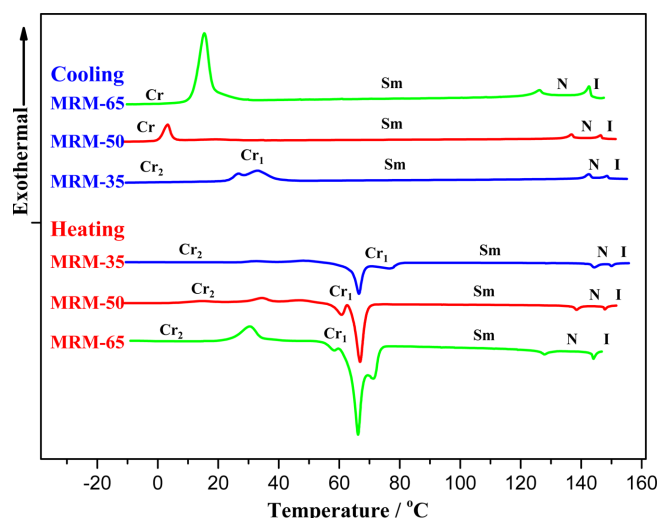


Figure 5. DSC thermograms of mixtures of SRM-1 and SRM-2 (MRM-65, MRM-50 and MRM-35 are mixtures of SRM-1 and SRM-2 with the weight % of SRM-1 is 65, 50, and 35%, respectively.).

transition temperature (T_{NS}) of the mixture decreased slightly with the addition of SRM-1 to SRM-2, the smectic-to-crystal phase transition temperature (T_{SC}) decreased significantly, which resulted in a wider smectic temperature range. For example, the mixture of SRM-1 and SRM-2 containing 65 wt% of SRM-1 (abbreviated as MRM-65) showed T_{NS} and T_{SC} at 128.0 and 20.8 °C, respectively, with the smectic temperature range of 107.2 °C. The mixture containing 50 wt% of SRM-1 (abbreviated as MRM-50) showed T_{SC} at 6.1 °C, which is lower than the room temperature. It should be noted that, contrary to the original SRMs, all the mixtures exhibited excellent alignment behavior on the rubbed alignment layer at either of nematic and smectic temperatures as shown in the POM images in Figure 6.

Therefore, MRM-50 (50 wt% of SRM-1) was chosen for the preparation of guest-host mixture because of its lowest crystallization point and superior aligning property. Firstly, appropriate amounts of dichroic dye (DAD, 1.5 wt%), thermal inhibitor (4-methoxypheno-

Table 2. Phase transition temperatures of SRM-1 and SRM-2^a

		Phase transition temperature				
MRM-35	Cooling (°C)	I 149.1	N 143.6	Sm 40.9	Cr	
	Heating (°C)	Cr 71.2	Sm 142.1	N 149.1	I	
MRM-50	Cooling (°C)	I 147.7	N 138.0	Sm 6.1	Cr	
	Heating (°C)	Cr 62.5	Sm 136.2	N 146.6	I	
MRM-65	Cooling (°C)	I 143.8	N 128.0	Sm 20.8	Cr	
	Heating (°C)	Cr 60.0	Sm 125.6	N 143.0	I	

^aI: Isotropic, N: Nematic, Sm: Smectic, Cr: Crystalline.

l, 0.2~0.3 wt%) and photo initiator (Irgarcure 369, 1.0 wt%) were mixed with the host LC mixture (MRM-50). Sandwich cells with 5 μm gap were prepared from two glass substrates in which both inner surfaces were coated with thin polyimide alignment layer (AL-16470, JSR Co.), uniaxially rubbed and antiparallely assembled. The guest-host mixture was injected into the cell by capillary action at 10-20 °C above the isotropic temperature. After slow cooling to the room temperature, a homogeneous planar alignment was obtained uniformly along the rubbing direction. Then, an *in-situ* photopolymerization was carried out *via* UV irradiation with an intensity of 10 mW·cm⁻² (@365 nm) at room temperature for an appropriate time period to achieve the stabilization of highly ordered smectic phase.

The optical property of the dye-doped MRM-50 mixture was investigated by polarized UV-vis spectra at various temperature, as shown in Figure 7. As can be seen in Figure 7(a), the absorbance spectra corresponding to the parallel and perpendicular directions to the polarizer were almost identical ($DR = 1$) at 155 °C as expected for isotropic liquid without molecular ordering. When the sample was cooled to nematic phase at 145 °C, the polarized UV-vis spectra in Figure 7(b) showed a significantly anisotropic absorption between parallel and perpendicular directions to the alignment direction, which indicates the dye molecules are co-aligned by the guest-host interaction between dye molecules and host MRM-50 mixture. The DR and S values were calculated to be 4.75 and 0.65, respectively, which agrees with those in nematic phase as previously reported.³³ Upon further cooling to

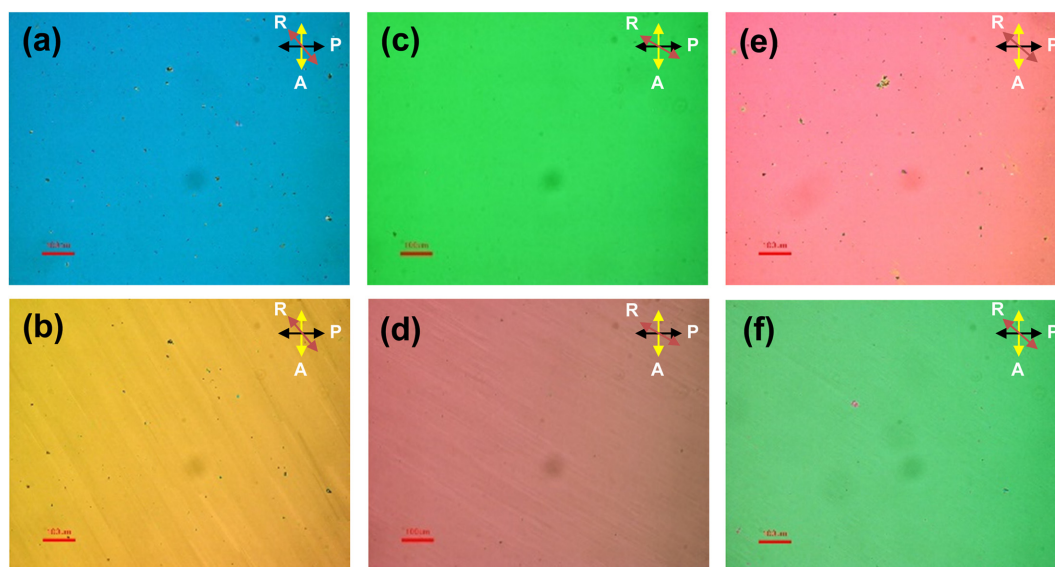


Figure 6. POM images of liquid crystal mixtures of SRM-1 and SRM-2 (sample is aligned in a rubbed sandwich cell). MRM-35 (a) at 143.7 °C and (b) at 110.7 °C; MRM-50 (c) at 139.7 °C and (d) at 72.7 °C; MRM-65 (e) at 140.5 °C and (f) at 90.7 °C.

smectic phase, the DR and S values increased significantly (DR = 36.1 and S = 0.92 at 25 °C) as displayed in Figure 7(c), indicating the highly ordered lamellar arrangement of the molecules in the smectic phase. Figure 7(d) summarizes the temperature dependent DR and S values obtained from the polarized UV-vis spectra of dye-doped MRM-50 mixture at various temperatures. At above the isotropic temperature (> 150 °C), DR and S values were 1 and 0, respectively, indicating a random orientation of dye molecules at isotropic temperature. When the sample was cooled to a nematic phase range, both DR and S increased slightly with S value increasing more dramatically than DR. Upon further cooling to a smectic phase range, DR and S increased continuously, and eventually, DR and S were measured to be 33 and 0.91 at room temperature. It should be noted that dye-doped MRM-50 mixture exhibits a smectic phase even at room tem-

perature during the cooling process due to the enantiotropic property, which is advantageous to obtain higher ordering of dye molecules.

When the photopolymerization of the orientated monomer mixture was carried out by UV irradiation at room temperature, the ordering of dye molecules decreased significantly due to the influence of photopolymerization as shown in Figure 8(a). The influence of polymerization on the ordering of dichroic dye molecules was depicted in Figure 8(b) in which DR and S values estimated from the polarized UV-Vis spectra during the photopolymerization process were plotted with respect to the curing time. With continuous UV irradiation, DR and S values decreased from 36.1 to 13.2 and from 0.92 to 0.80, respectively, and finally reached a steady stage after 15 min. These significant decreases are possibly attributed to the disordering of mesogenic cores in

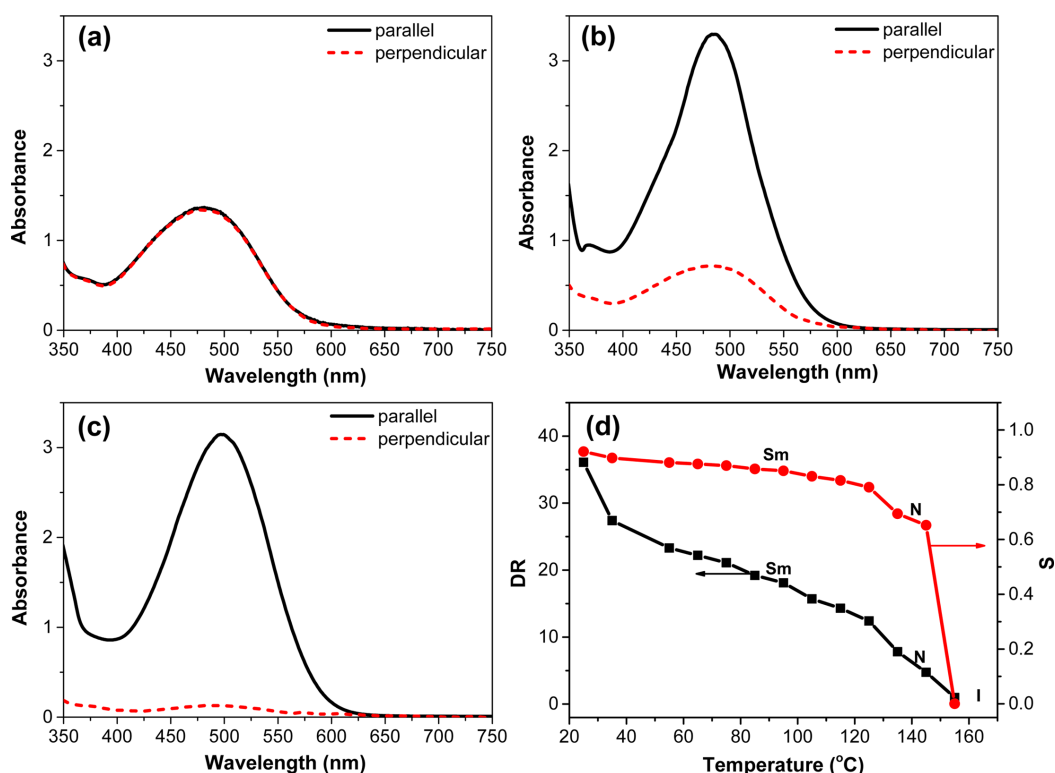


Figure 7. Polarized UV-vis spectra of MRM-50 mixture: (a) at 155 °C (DR = 1.0, S = 0), (b) at 145 °C (DR = 4.8, S = 0.652) and (c) at 25 °C (DR = 27.4, S = 0.898). Solid and dotted lines correspond to absorption in parallel and perpendicular directions to the polarizer, respectively. (d) DR and S vs. temperature for MRM-50 mixture.

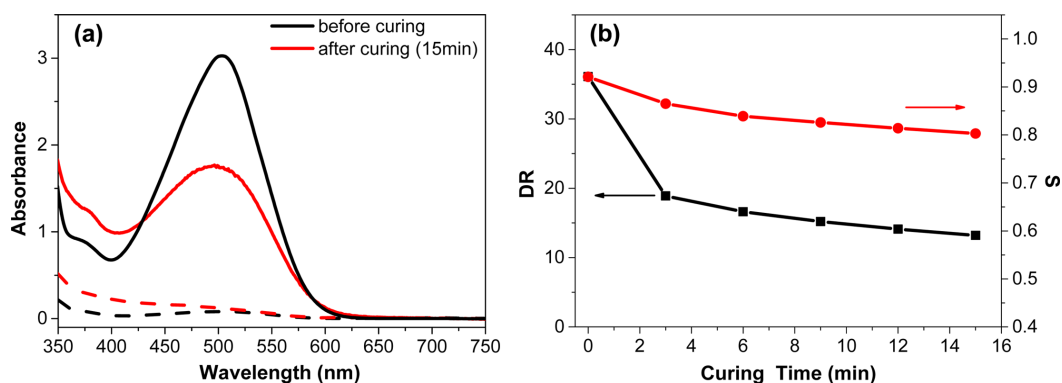


Figure 8. (a) Polarized UV-vis spectra of MRM-50 mixture before (black) and after (red) UV curing process for 15 mins. Solid and dotted lines correspond to absorption in parallel and perpendicular directions to the polarizer, respectively. (b) DR (black) and S (red) vs. UV curing time for MRM-50 mixture.

the polymer network induced by the configurational change of acrylate terminal from sp^2 to sp^3 and the volume shrinkage during the polymerization of acrylate groups.^{23,34-37} Based on the above results, the photopolymerization was performed for 15 min to ensure a sufficient photopolymerization, which gives DR = 13.2 and S = 0.80, respectively. A degree of polarization (DOP) was also calculated from the Eq. (3) to be 95.5% (@496.2 nm) with the thickness of 5 μm .

4. Conclusions

We designed and synthesized two new calamitic liquid crystal-line monomers (SRM-1 and SRM-2) containing photopolymerizable acrylate groups. The structures of monomers were characterized by ^1H NMR spectroscopy, and their mesomorphic behaviors were investigated by DSC and POM. Both of SRM-1 and SRM-2 showed an enantiotropic phase transition behavior with exhibiting both nematic phase and highly ordered smectic phase. In the case of SRM-1, during the cooling process, both nematic and smectic phases were observed in the temperature range of 144.2–94.0 °C and 94.0–47.8 °C, respectively. Especially, SRM-1 was strongly believed to possess a smectic C (SmC) phase among many other smectic phases. In the case of SRM-2, a nematic phase was observed only in a very short temperature range (155.9–154.0 °C) followed by a smectic phase in the temperature range of 154.0–85.8 °C, and two crystalline phases below 85.8 °C. Neither of the SRMs showed a homogeneous alignment even at various temperatures, so that the mixtures of SRM-1 and SRM-2 with different weight ratios were subjected to further investigation for the purpose of fabrication of guest-host thin film polarizers. Among the mixtures, 50:50 mixture of SRM-1 and SRM-2 (MRM-50) was chosen for the preparation of guest-host mixture because of its lowest crystallization point and superior aligning property. After adding a dichroic dye, photoinitiator, and other additives, the guest-host mixture was injected into a sandwich cell containing rubbed alignment layers. The dichroic ratio (DR) and order parameter (S) were measured to be 36.1 and 0.92, respectively, which are much higher than those of nematic phase guest-host systems. Then, *in-situ* photopolymerization was carried out *via* UV irradiation at room temperature to achieve the stabilization of highly ordered smectic phase. Upon photopolymerization, the decrease of DR and S was unavoidable due to the disordering of mesogenic cores which was probably induced by the configurational change of acrylate terminal and the volume shrinkage during the polymerization. Nonetheless, the dichroic ratio, order parameter and degree of polarization (DOP) were measured to be 13.1, 0.80 and 95.5% (@496.2 nm), respectively. In conclusion, the new reactive liquid crystalline monomers synthesized in this work possess highly ordered smectic phase with wide smectic phase temperature range and low crystallization temperature, which could be promising host materials for the preparation of guest-host type coatable polarizers.

References

(1) P. Yeh and C. Gu, *Optics of Liquid Crystal Displays*, John Wiley & Sons, New Jersey, 2010.

- (2) K. J. Gåsvik, in *Optical Metrology*, John Wiley & Sons, West Sussex, England, 2003, pp 219–221.
- (3) X.-L. Ma, X.-C. Chen, L. Xiao, H.-Y. Wang, J.-F. Tan, P. Song, G. Shi, Y.-F. Yang, J. Lv, and D.-W. Wang, *SID Symp. Digest*, **48**, 1735 (2017).
- (4) E. H. Land, *J. Opt. Soc. Am.*, **41**, 957 (1951).
- (5) M. M. Zwick, *J. Polym. Sci. Part A-1: Polym. Chem.*, **4**, 1642 (1966).
- (6) J. G. Pritchard and D. A. Akintola, *Talanta*, **19**, 877 (1972).
- (7) W. J. Gunning and J. Foschaar, *Appl. Opt.*, **22**, 3229 (1983).
- (8) K. Miyasaka, *Adv. Polym. Sci.*, **108**, 91 (1993).
- (9) T. Yokoyama, K. Kaneyuki, H. Sato, H. Hamamatsu, and T. Ohta, *Bull. Chem. Soc. Jpn.*, **68**, 469 (1995).
- (10) W. Lyoo, J. Yeum, H. Ghim, J. Park, S. Lee, J. Kim, D. Shin, and J. Lee, *Colloid Polym. Sci.*, **281**, 416 (2003).
- (11) E. J. Shin, Y. H. Lee, and S. C. Choi, *J. Appl. Polym. Sci.*, **91**, 2407 (2004).
- (12) H. Mori, *IMID'05 Digest*, 1071 (2005).
- (13) F. Chimera, *Flat Panel Display Materials: Trends and Forecasts 2009*, Interlingua Publishing, Redondo Beach, 2009.
- (14) S.-M. Lee, J. H. Kwon, S. Kwon, and K. C. Choi, *IEEE Trans. Elect. Devices*, **64**, 1922 (2017).
- (15) E. Peeters, J. Lub, J. A. M. Steenbakkens, and D. J. Broer, *Adv. Mater.*, **18**, 2412 (2006).
- (16) T. Sergan, T. Schneider, J. Kelly, and O. D. Lavrentovich, *Liq. Cryst.*, **27**, 567 (2000).
- (17) R. Piñol, J. Lub, M. P. García, E. Peeters, J. L. Serrano, D. Broer, and T. Sierra, *Chem. Mater.*, **20**, 6076 (2008).
- (18) S.-K. Park, S.-E. Kim, D.-Y. Kim, S.-W. Kang, S. Shin, S.-W. Kuo, S.-H. Hwang, S. H. Lee, M.-H. Lee, and K.-U. Jeong, *Adv. Funct. Mater.*, **21**, 2129 (2011).
- (19) P. Im, D.-G. Kang, D.-Y. Kim, Y.-J. Choi, W.-J. Yoon, M.-H. Lee, I.-H. Lee, C.-R. Lee, and K.-U. Jeong, *ACS Appl. Mater. Interfaces*, **8**, 762 (2016).
- (20) H. Lu, Q. Zhang, J. Sha, M. Xu, J. Zhu, G. Zhang, Y. Ding, and L. Qiu, *Liq. Cryst.*, **46**, 1574 (2019).
- (21) V. G. Rumyantsev, A. V. Ivashchenko, V. M. Muratov, V. T. Lazareva, E. K. Prudnikova, and L. M. Blinov, *Mol. Cryst. Liq. Cryst.*, **94**, 205 (1983).
- (22) P. J. Collings, M. Hird, in *Introduction to Liquid Crystals: Chemistry and Physics*, CRC Press, Philadelphia, 2017, pp 43–46.
- (23) R. He, E. Oh, Y. Ye, P. Wen, K.-U. Jeong, S. H. Lee, X.-D. Li, and M.-H. Lee, *Polymer*, **176**, 51 (2019).
- (24) A. V. Ivashchenko, *Dichroic Dyes for Liquid Crystal Displays*, CRC Press, 2018, Ch. 1.
- (25) G. Höfle, W. Steglich, and H. Vorbrüggen, *Angew. Chem. Int. Ed.*, **17**, 569 (1978).
- (26) B. Neises and W. Steglich, *Angew. Chem. Inter. Ed.*, **17**, 522 (1978).
- (27) A. Hassner and V. Alexanian, *Tetrahedron Lett.*, **19**, 4475 (1978).
- (28) K. Sonogashira, Y. Tohda, and N. Hagihara, *Tetrahedron Lett.*, **17**, 4467 (1975).
- (29) K. Sonogashira, *J. Organomet. Chem.*, **653**, 46 (2002).
- (30) K. T. Wong, F. C. Fang, Y. M. Cheng, P. T. Chou, G. H. Lee, and Y. Wang, *J. Org. Chem.*, **69**, 8038 (2004).
- (31) H. Sackmann and D. Demus, *Mol. Cryst.*, **2**, 81 (1966).
- (32) I. Dierking, in *Textures of Liquid Crystals*, John Wiley & Sons, 2003, pp 91–122.
- (33) D. Demus, J. W. Goodby, and G. W. Gray, *Handbook of Liquid Crystals, Volume 2A: Low Molecular Weight Liquid Crystals I: Calamitic Liquid Crystals*, John Wiley & Sons, 2011.
- (34) C. J. Kleverlaan and A. J. Feilzer, *Dent. Mater.*, **21**, 1150 (2005).
- (35) C. J. Drury, C. M. J. Mutsaers, C. M. Hart, M. Matters, and D. M. de Leeuw, *Appl. Phys. Lett.*, **73**, 108 (1998).
- (36) N. B. Cramer, J. W. Stansbury, and C. N. Bowman, *J. Dent. Res.*, **90**, 402 (2010).
- (37) E. Smela and L. J. Martínez-Miranda, *J. Appl. Phys.*, **73**, 3299 (1993).

Publisher's Note Springer Nature remains neutral with regard to jurisdictional claims in published maps and institutional affiliations.